

On the influence of simulated SST warming on rainfall projections in the Indo-Pacific domain: an AGCM study

Huqiang Zhang¹  · Y. Zhao^{2,3} · A. Moise¹ · H. Ye¹ · R. Colman¹ · G. Roff¹ · M. Zhao¹

Received: 18 October 2016 / Accepted: 13 April 2017 / Published online: 21 April 2017
© Springer-Verlag Berlin Heidelberg 2017

Abstract Significant uncertainty exists in regional climate change projections, particularly for rainfall and other hydro-climate variables. In this study, we conduct a series of Atmospheric General Circulation Model (AGCM) experiments with different future sea surface temperature (SST) warming simulated by a range of coupled climate models. They allow us to assess the extent to which uncertainty from current coupled climate model rainfall projections can be attributed to their simulated SST warming. Nine CMIP5 model-simulated global SST warming anomalies have been super-imposed onto the current SSTs simulated by the Australian climate model ACCESS1.3. The ACCESS1.3 SST-forced experiments closely reproduce rainfall means and interannual variations as in its own fully coupled experiments. Although different global SST warming intensities explain well the inter-model difference in global mean precipitation changes, at regional scales the SST influence vary significantly. SST warming explains about 20–25% of the patterns of precipitation changes in each of the four/five models in its rainfall projections over the oceans in the Indo-Pacific domain, but there are also a couple of models in which different SST warming explains little of their precipitation pattern changes. The influence is weaker again for rainfall changes over land. Roughly similar levels of contribution can be attributed to

different atmospheric responses to SST warming in these models. The weak SST influence in our study could be due to the experimental setup applied: superimposing different SST warming anomalies onto the same SSTs simulated for current climate by ACCESS1.3 rather than directly using model-simulated past and future SSTs. Similar modelling and analysis from other modelling groups with more carefully designed experiments are needed to tease out uncertainties caused by different SST warming patterns, different SST mean biases and different model physical/dynamical responses to the same underlying SST forcing.

1 Introduction

Increasing observational evidence presented by a series of Intergovernmental Panel for Climate Change (IPCC) Assessment Reports (available online at <http://www.ipcc.ch/>) has shown unequivocal climate change signals across the globe. Partly in response to the impacts of such climate changes, regional climate change projections are in high demand. Nevertheless, a fundamental limitation on the utility of current projections is that there are still large uncertainties on regional scales (IPCC 2007, 2013), particularly for rainfall projections (Xie et al. 2010; Hawkins and Sutton 2011). As highlighted in Curry and Webster (2011), understanding and reducing such uncertainties is critical given their significant implications for the science–policy interface and its socioeconomic importance.

A large number of studies have sought to link the uncertainty in rainfall projections to different underlying SST warming in the tropics. They found coupled model-simulated changes in tropical Pacific precipitation were tied to changes in the underlying SST patterns and/or intensities (Xie et al. 2010; Kent et al. 2015; Grose et al. 2014;

✉ Huqiang Zhang
h.zhang@bom.gov.au

¹ Bureau of Meteorology, GPO Box 1289K, Melbourne, VIC 3001, Australia

² School of Atmospheric Sciences, Chengdu University of Information Technology, Chengdu, China

³ Institute of Desert Meteorology, China Meteorological Administration, Xinjiang, China

Chadwick et al. 2013, 2014, 2017; Brown et al. 2016; Chadwick 2016; He and Soden 2016). Some of these studies showed that regions with large uncertainties in projections were co-located with large discrepancies in simulated SST changes (Grose et al. 2014; Kent et al. 2015; Brown et al. 2015). A recent study by Brown et al. (2016) divided CMIP5 models into dry/wet/mid subgroups in terms of their projected rainfall changes of the Australian monsoon. They found dry models tend to have a large cold bias in their present day western equatorial Pacific SSTs and the wet models to have largest warming in the central and eastern equatorial Pacific. Chadwick (2016) and He and Soden (2016) suggested that different SST patterns contributed more uncertainties in rainfall projections in tropical oceans but SST biases or warming intensities were important for uncertainty over land. Our previous studies (Zhang et al. 2012, 2013, 2016; Dong et al. 2015), also showed influences of SST warming in tropical Pacific and Indian oceans on inter-model differences in CMIP3 and CMIP5 model-simulated changes in the Asian and Australian monsoons and climate in central Asia (Zhao and Zhang 2016).

Besides the recognition of the influence of SST warming on regional rainfall projections, there are also studies emphasising that different atmospheric circulation responses to global warming are another major source of uncertainty (Shepherd 2014). This is because rainfall is the product of atmospheric dynamics interacting with moisture conditions (Zhang 2010). For instance, Colman et al. (2011) used 500 hPa vertical velocity to examine Australian monsoon rainfall generation by decomposing total precipitation into two components: one is the relative occurrence of particular convective regimes and the other is how much precipitation on average falls per vertical motion regime. They reported that models overestimating summer rainfall tended to have stronger westerlies and were systematically more ‘convective’. In contrast, models with underestimated monsoon rainfall showed not just suppressed regional convection, but too little precipitation for all convective and suppressed conditions. Moise et al. (2012) further decomposed projected rainfall changes and showed uncertainty associated with model dynamical processes. Shepherd (2014) concluded that limited confidence in atmospheric circulation aspects of climate change lead to uncertainty in model projections of circulation-related fields such as precipitation.

Therefore, more thorough statistical and modelling studies are needed to dismantle such complex linkages between SST warming and atmospheric responses under a range of modelling configurations. In this study we conduct AMIP-type (Atmospheric Model Intercomparison Project) SST experiments using a single climate model, which has reasonable tropical rainfall-SST connections

compared with observations (see below). We force the model with different SST warming projected by a group of CMIP5 models to assess their contributions to regional projections. The utility of these AMIP-type experiments has already been demonstrated by several studies. For example, Zhou et al. (2014) conducted experiments using a single AGCM forced with its simulated SST warming and compared with CMIP5 models “amip4K” and “amip-Future” ensembles (Taylor et al. 2012). They found this approach could reproduce the potential changes of ENSO impacts on global climate under a warmed climate. By super-imposing SST warming simulated by a CMIP5 model onto both observed SSTs and model-simulated SST climatology, Zhou and Xie (2015) showed the impacts of climatological model SST biases on projecting tropical climate change. Recent AMIP-type studies such as Brown et al. (2015), He and Soden (2016) also provided valuable results on exploring the contributions from SST warming patterns and biases in rainfall projections. By super-imposing SST warming from nine different CMIP5 models onto a single AGCM under different greenhouse gas (GHG) concentrations (current and future), our experiments are complementary to these aforementioned studies by offering the following features:

1. Applying different SST warming from different CMIP5 model simulations to the same AGCM—in contrast to the same SST warming to different AGCMs as used in CMIP5 amip4K and amipFuture (e.g., Zhou et al. 2014; Zhou and Xie 2015). Therefore, we can quantify the uncertainty caused by SST warming under the same atmospheric model physics/dynamics in a simple and clean way such as He and Soden (2016) did. As SST-rainfall connections can be different among the models as to be discussed later, our modelling experiments will also help to assess the model-dependence of these published results;
2. Applying the different SST warming to the model under two different GHG concentrations (current and *RCP4.5*) allows us to assess whether under different GHG radiative forcing the influence from different SST warming patterns/intensities varies as discussed in Chadwick (2016).

Accordingly, the manuscript is arranged as follows: Sect. 2 describes the experimental design and the CMIP5 model results used in the analysis. Detailed analysis of the AGCM AMIP-type experiments is presented in Sect. 3, including results under different GHG concentrations. Section 4 contains conclusion and discussions on the limitations in this analysis and some future plans.

2 Experimental design and analytical methods

2.1 ACCESS1.3

In this study, we use the Australian Community Climate and Earth-System Simulator (ACCESS) AGCM version 1.3 for conducting the SST-forced experiments. The coupled version of ACCESS1.3 participated in the CMIP5 coupled experiments while it also contributed uncoupled AMIP experiment to CMIP5. The model showed competitive skill for Australian (Watterson et al. 2013) and tropical climate (Grose et al. 2014). Detailed descriptions of the physics and dynamics of the model are given in Bi et al. (2013), and references therein. The ACCESS1.3 AGCM was based on the UK Met Office Global Atmosphere 1.0 configuration (Hewitt et al. 2011) with the PC2 cloud scheme (Wilson et al. 2008), but coupled to an Australia-developed land surface model named CABLE (Kowalczyk et al. 2013), together with some other modifications as detailed in Bi et al. (2013). The model has a horizontal

resolution of 1.25° latitude by 1.875° longitude (referred to as ‘N96’) and 38 vertical levels.

Given that focus of this study is the impact of SST warming on CMIP5 model rainfall projections, we first need to evaluate whether ACCESS1.3 SST-rainfall correlations in the tropics are close to observed. Figure 1 shows such results from its coupled *historical* run for the period of 1971–2000 versus the observational results derived from the Global Precipitation Climatology Project (GPCP) rainfall of Huffman et al. (2009) and SSTs of Smith and Reynolds (2003) for the period of 1979–2009. The coupled ACCESS1.3 can, by and large, simulate many of the observed features such as the strong SST-rainfall correlation in the central and eastern tropical Pacific while negative correlations in the tropical eastern Indian Ocean and part of the maritime continent (except for the months in Jun/Jul–Oct). Such contrast is largely due to specific air–sea coupling characteristics in the tropics. SST warming in the tropical eastern Pacific leads to more atmospheric convection and rainfall. While in the eastern tropical Indian Ocean

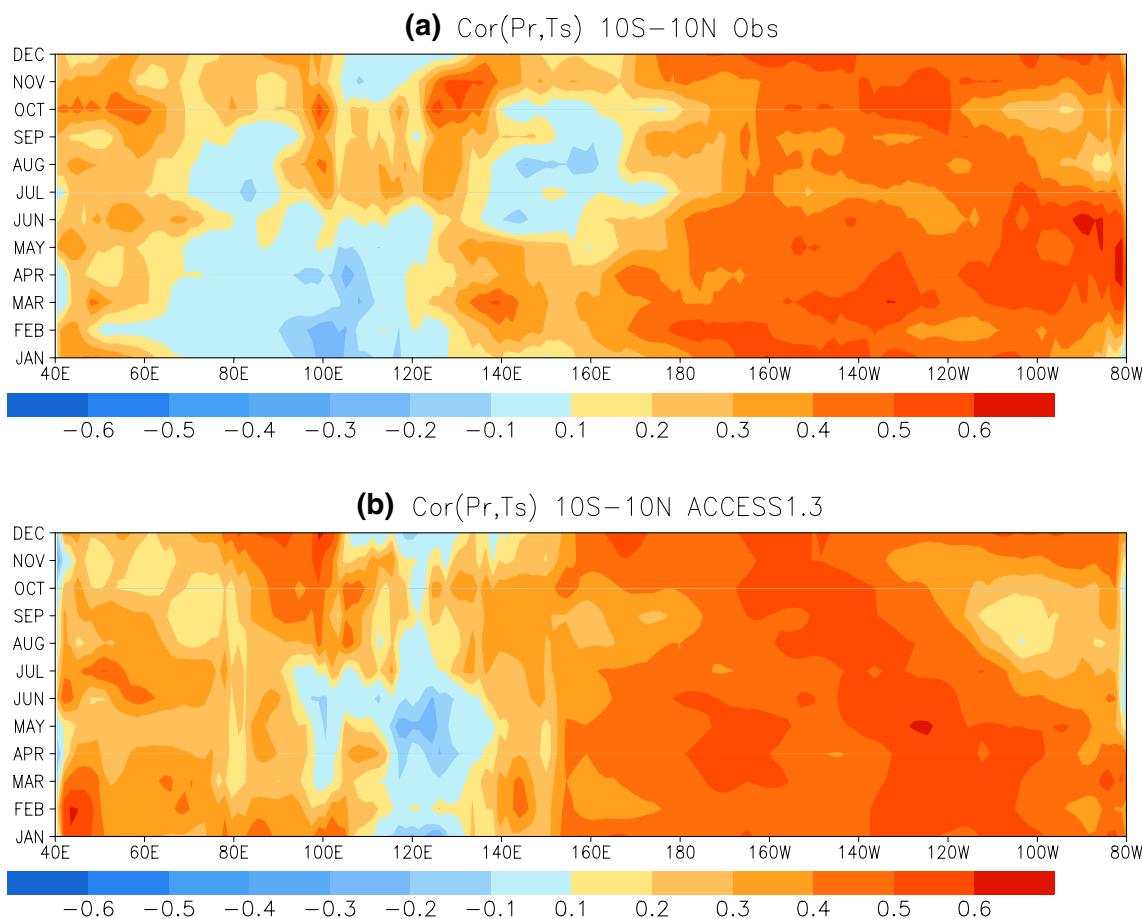


Fig. 1 a Averaged point-to-point correlations between SST and rainfall in the deep tropics (10°S–10°N) in observational data (with SST of Smith and Reynolds (2003) and GPCP (Huffman et al. 2009) rain-

fall for the period of 1979–2009). Correlations are calculated after first removing the annual cycle; b as a but from ACCESS1.3 CMIP5 historical run for the period of 1971–2000

negative SST-rainfall correlation in the austral summer season reflects the SSTs in this region respond to the change in atmospheric forcing as discussed in Bollasina and Nigam (2009), Hendon et al. (2011) and Zhang and Moise (2016). In this regard, ACCESS1.3 shows skill in capturing the overall fundamental features and is generally more skilful than other models as shown in Fig. 2 which compares with the other eight models used in this study. Details of these models are provided in the next section. There are large differences across the nine models, with some models including ACCESS1.3, CNRM-CM5, GFDL-ESM2G and HadGEM3-CC having much stronger and much extended correlations between SST and rainfall east of the dateline than others. ACCESS1.3 has generally stronger positive responses of (deep) tropical rainfall to underlying SST conditions at virtually all longitudes. Therefore, if different SST warming patterns/intensities play a key role leading to discrepancies in the CMIP5 model-simulated tropical rainfall changes, one might expect a clear signal in ACCESS1.3 SST experiments. These results provide confidence in using ACCESS1.3 AGCM for assessing such impacts although we acknowledge that correlations between rainfall/regional SSTs in these models can differ from ACCESS1.3 in some months and regions.

2.2 ACCESS1.3 SST experiments

Table 1 lists the series of SST experiments performed. Unless indicated otherwise, all the experiments in this study are integrated for 30 years to achieve stable and statistically meaningful results. The experiments are:

ACCESSsst_his Forcing the ACCESS1.3 AGCM with SSTs from its coupled version CMIP5 *historical* run for 1971–2000. Its monthly SST values are linearly interpolated into daily fields over the course of the model integration. The GHG concentrations and other forcings are as specified in the *historical* experiment (Taylor et al. 2012).

ACCESSsst_rcp Forcing the AGCM with SSTs from coupled ACCESS1.3 *RCP8.5* run for 2070–2099, but with GHG and aerosol concentrations from *RCP4.5* which represents a moderate increase in GHG concentration. The reason for using *RCP4.5* rather than *RCP8.5* is that we try to give a relatively weaker GHG radiative forcing constrains to the model so the SST influence across the models can be identified more easily. As discussed below, we have also conducted experiments with no increase in GHG concentrations.

SST_exp Superimposing monthly SST climatological anomalies simulated by the nine CMIP5 models listed

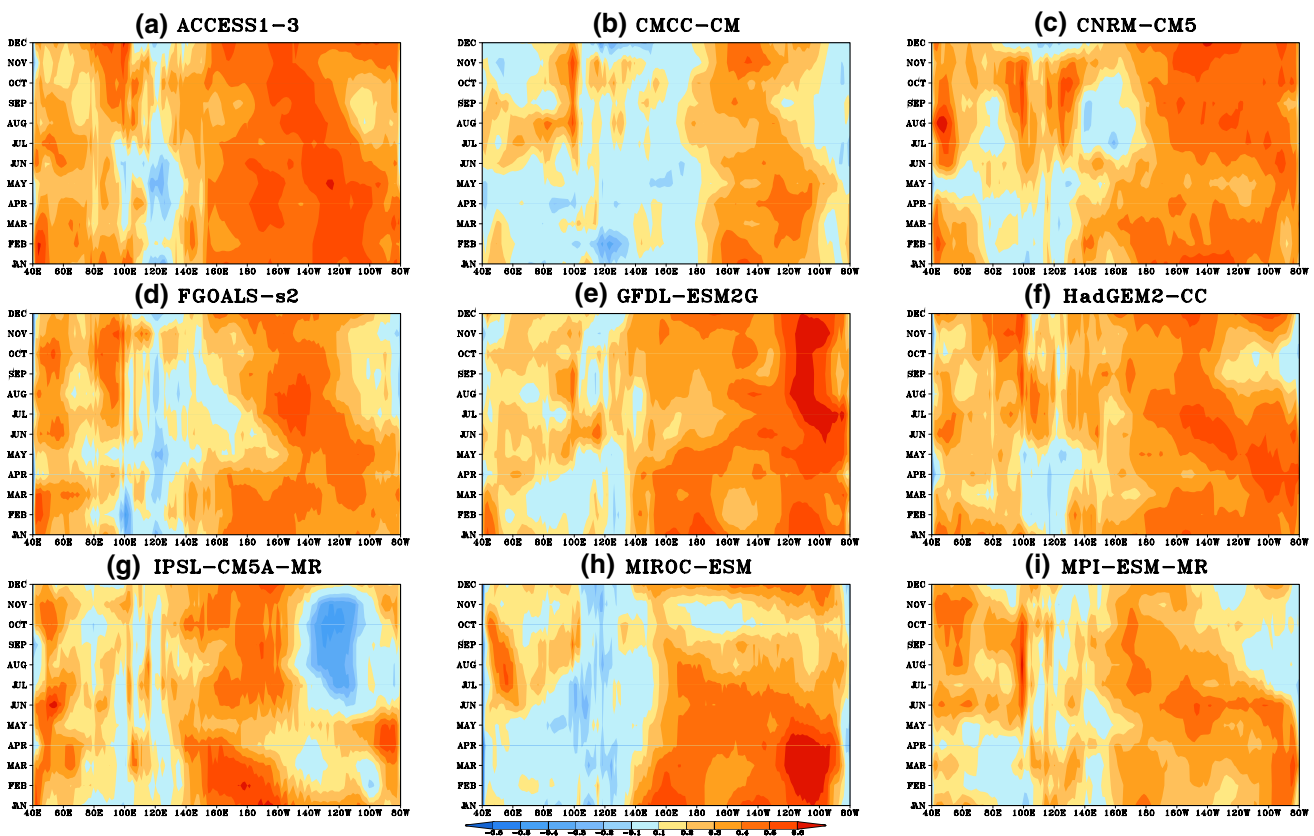


Fig. 2 As Fig. 1b but for comparing ACCESS1.3 results against eight other models as listed in Table 1

Table 1 ACCESS1.3 AMIP-type experiments conducted and analysed in the study

Experiment ID	Period	Specified SSTs	Greenhouse gases
<i>ACCESSsst_his</i>	1971–2000	Monthly SSTs from ACCESS1.3 CMIP5 <i>historical</i> coupled run	Time-varying GHG concentration as used in CMIP5 <i>historical</i> runs
<i>ACCESSsst_rcp</i>	2070–2099	Monthly SSTs from ACCESS1.3 CMIP5 <i>RCP8.5</i> coupled run	GHG concentration as used in CMIP5 <i>RCP8.5</i> runs
<i>SST_exp</i> for nine models: ACCESS1.3, CMCC-CM, CNRM-CM5, FGOALS-s2, GFDL-ESM2G, HadGEM2-CC, IPSL-CM5A-MR, MIROC-ESM, MPI-ESM-MR, with model numbered from 1 to 9 accordingly	2070–2099	Superimposing 30 year monthly mean SST anomalies derived from each model's <i>RCP8.5</i> (2070–2099) and <i>historical</i> (1971–2000) runs onto the monthly SST time series simulated by ACCESS1.3 <i>historical</i> run for the period of 1971–2000. Changes are derived as the differences between <i>SST_exp</i> against <i>ACCESSsst_his</i>	GHG concentration as used in CMIP5 <i>RCP4.5</i> runs
<i>SSTghg_exp</i> for nine models: ACCESS1.3, CMCC-CM, CNRM-CM5, FGOALS-s2, GFDL-ESM2G, HadGEM2-CC, IPSL-CM5A-MR, MIROC-ESM, MPI-ESM-MR	2070–2099	As for <i>SST_exp</i> Changes are derived as the differences between <i>SST_exp</i> against <i>ACCESSsst_his</i>	GHG concentration as used in CMIP5 <i>historical</i> runs
CMIP5 experiments analysed: <i>CMIP5_exp</i> for nine models: ACCESS1.3, CMCC-CM, CNRM-CM5, FGOALS-s2, GFDL-ESM2G, HadGEM2-CC, IPSL-CM5A-MR, MIROC-ESM, MPI-ESM-MR	1971–2000 (<i>historical</i>) and 2070–2099 (<i>RCP8.5</i>)	Fully coupled CMIP5 experiments	<i>Historical</i> <i>RCP8.5</i>

in Table 1 onto the monthly SST time series simulated by ACCESS1.3 coupled *historical* run over the period of 1971–2000. The monthly SST warming in these nine models is derived from their *RCP8.5* experiments averaged over the period of 2070–2099 against their *historical* runs (1971–2000). The nine models are selected based on our analysis of Australian and Asian monsoon in CMIP5 simulations (Dong et al. 2015; Zhang et al. 2016) in which these models tended to represent the scatter among over 25 models analysed, and showed strong differences in their model-simulated tropical SST warming. In the *SST_exp* experiments, the lower GHG concentrations in *RCP4.5* are used as to reduce the effect that the model sensitivity to different SST warming may be overshadowed by a large GHG imposed radiative forcing.

SSTghg_exp As *SST_exp* but using the GHG concentrations and aerosols as in CMIP5 *historical* runs, i.e., only SST warming but no increases in GHG and aerosol concentrations. This is used to assess the relative contributions from SST warming and GHG radiative forcing to rainfall projections and associated uncertainties as discussed in Chadwick (2016).

As a first step, we need to examine whether AMIP-type SST experiments using ACCESS1.3 provide a valid approach, in that they can replicate the main climate change signals simulated in its own fully coupled runs. Figure 3 compares the coupled ACCESS1.3 simulated changes in surface skin temperature (i.e., SST for open ocean) between its *RCP8.5* (2071–2100) and *historical* (1971–2000) runs in January and July against those from its SST experiments (*ACCESSsst_his* and *ACCESSsst_rcp*). The high similarity over the oceans between the two sets of runs (cannot be identical due to interpolations used in generating ancillary files) demonstrates that the technical setup is properly done for superimposing model-simulated SST anomalies onto the SST time series in its *control* experiment. The differences over land reflect land-air interactions where there are no constraints on soil temperature in both coupled and *SST_exp* configurations. Furthermore, Fig. 4 shows that the AGCM driven by monthly SST warming anomalies from its coupled runs can largely reproduce the dominant patterns of rainfall changes and their intensities as in its coupled runs. The spatial correlations between these two sets of experiments are 0.83 (DJF) and 0.92 (JJA) for the

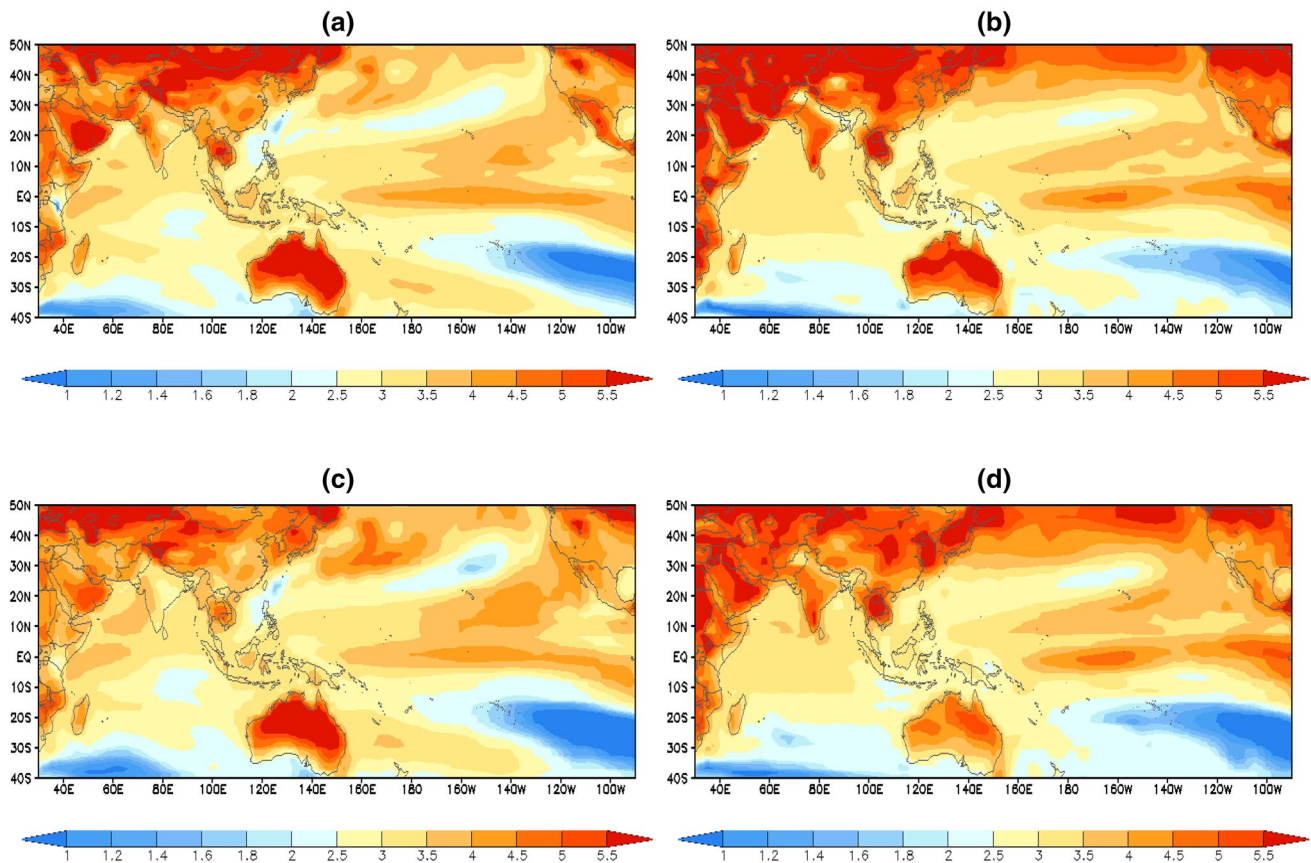


Fig. 3 DJF (a, c) and JJA (b, d) surface temperature differences (°C) derived from ACCESS1.3 CMIP5 experiments (a, b) and the corresponding results from its SST runs derived from *ACCESSsst_rcp* and *ACCESSsst_his* (c, d)

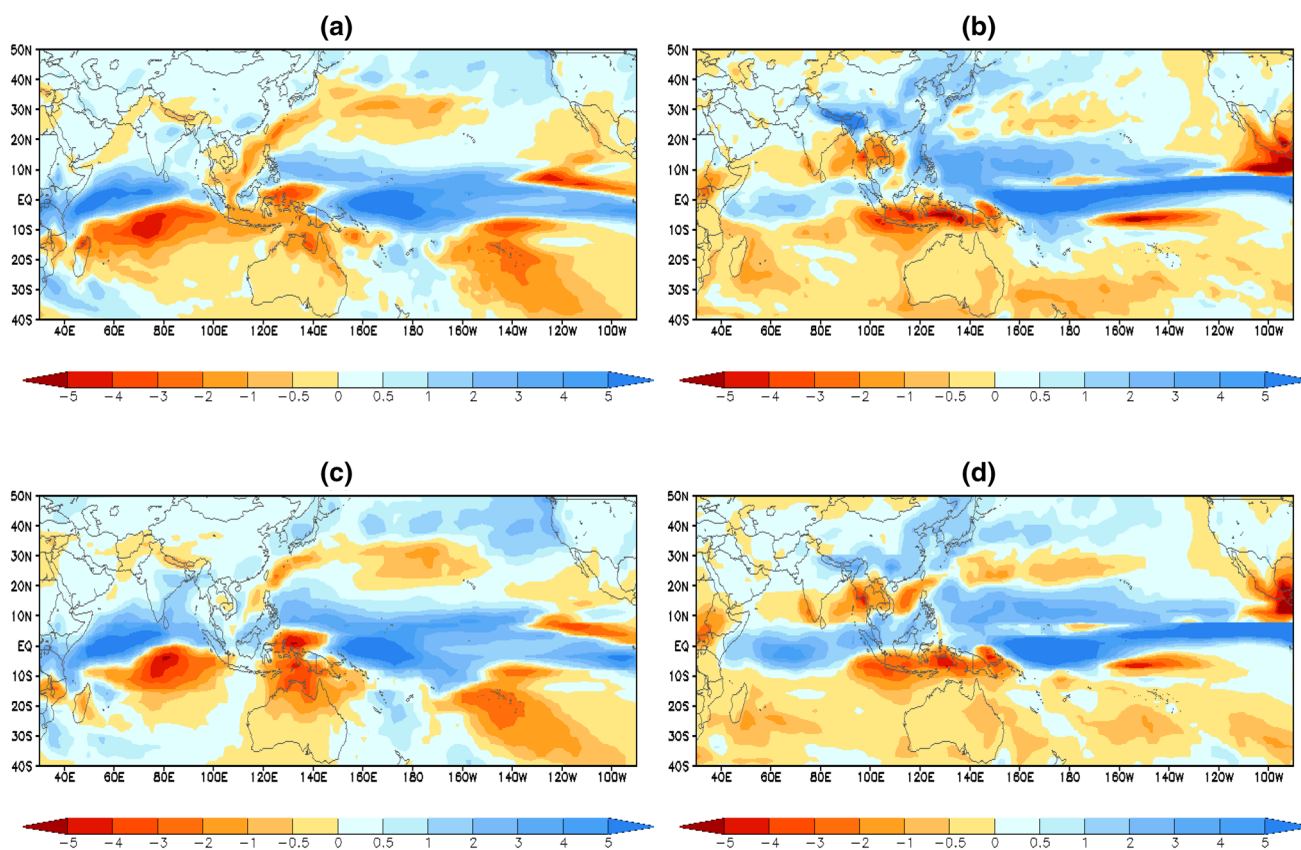


Fig. 4 As Fig. 3 but for rainfall changes (mm d^{-1})

Indo-Pacific domain of 30° – 270° E and 40° S– 50° N. This is the main domain focused on in our analysis.

Overall results presented in Figs. 1, 2, 3 and 4 provide confidence in the experimental setup used in these sensitivity studies. In addition, to keep the manuscript concise, we focus on showing some detailed results in DJF for most cases when the Australian summer monsoon peaks.

3 Results

3.1 Model uncertainty in the fully coupled CMIP5 runs

First we examine how different the nine CMIP5 models are in their simulated rainfall changes in the Indo-Pacific domain (Fig. 5). Note that to well capture the patterns of rainfall changes, we use rainfall changes in percentage in Fig. 5. There are notable common features among the models, including rainfall increases in the eastern tropical Pacific and decreases to its north and south. However, large disagreements are evident at regional scales, primarily in the western tropical Pacific and tropical and southern Indian Oceans. Some of the results have been well documented in other studies, such as Brown et al. (2013) and

Brown et al. (2016) on the modelled rainfall projections in the Southern Pacific convergence zone (SPCZ).

Figure 6 shows the DJF surface skin temperature (i.e., SST for open ocean) warming simulated by these nine models. While all the models show substantial warming with increased GHG concentrations, the intensity and patterns differ. Over the tropical oceans, a number of the models (including ACCESS1.3, FGOALS_s2, MRCC_ESM and IPSL_CM5A-MR) show enhanced warming over the eastern tropical Pacific, often referred to as ‘El Nino-like warming’ as documented by many studies (Yeh et al. 2012; Song and Zhang 2014). A number of models, however, do now show such notable features (such as CNRM-CM5 and GFDL-ESM2G).

At global scale, changes in global mean precipitation are primarily govern by the changes in atmospheric energy balance in the models and many studies have confirmed the linkage between warming intensity in the CMIP5 models and rainfall changes (e.g., Allen and Ingram 2002). This is shown in Fig. 7a for both DJF and JJA seasons. The more intense warming simulated by the model, the more global rainfall increases through enhanced hydrological cycle in warmed climate (Held and Soden 2005; Lavers et al. 2015). This explains about 73% of the spread among the

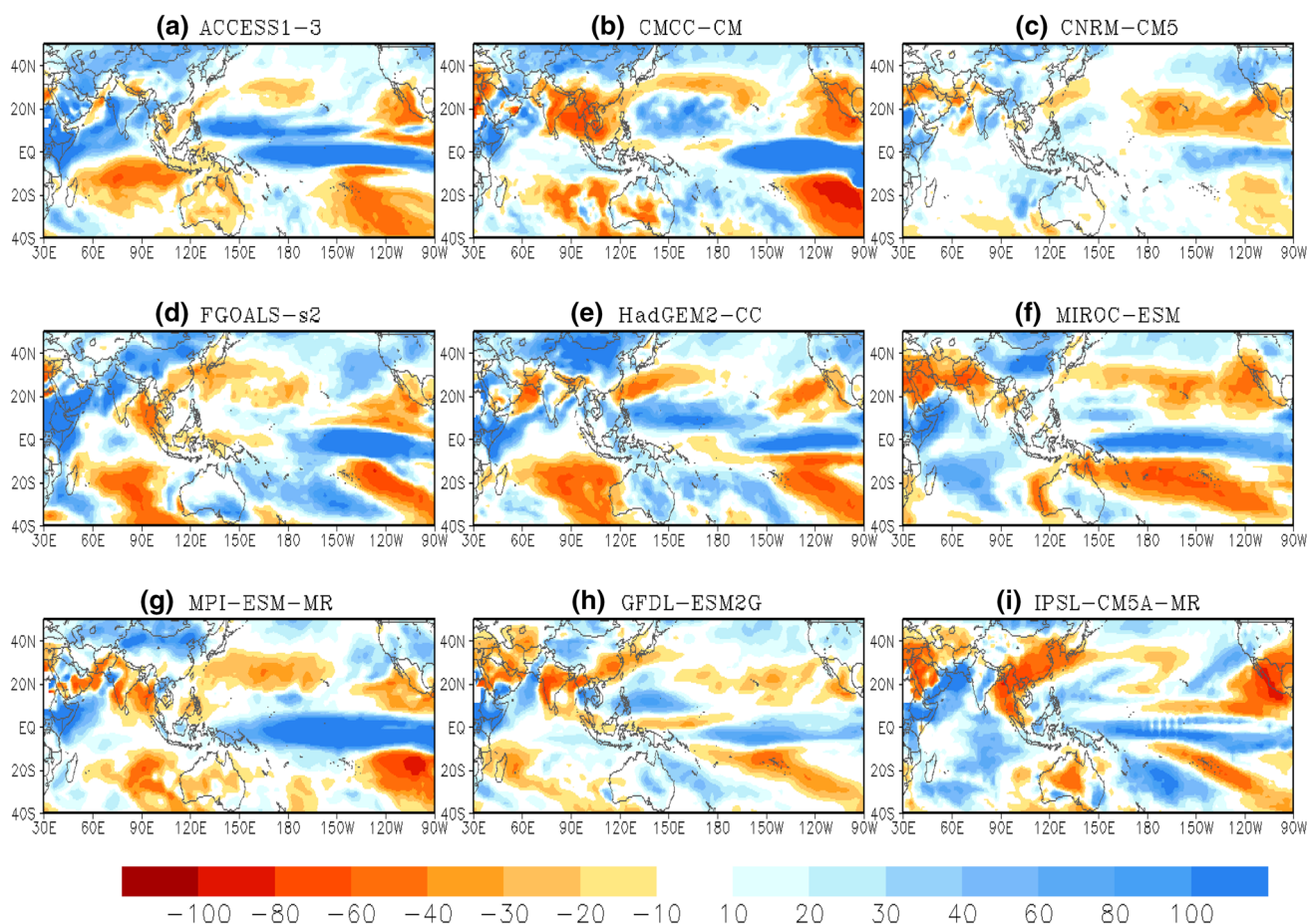


Fig. 5 DJF rainfall changes (%) from the nine models CMIP5 simulations. Precipitation changes are the mean differences between their *RCP8.5* runs for 2070–2099 and the historical runs for 1971–2000

models in their globally averaged quantities. This relationship also holds for the superimposed SST warming onto the ACCESS1.3 historical SSTs—i.e., the results from the *SST_exp* experiment (Fig. 7b). This demonstrates the forced AGCM *SST_exp* runs can largely reproduce the spread of globally-averaged rainfall changes from the corresponding coupled runs. The correlation between the two set of rainfall projections is 0.84, reproducing around 70% the inter-model variations. In the next section, we will focus on the replication of rainfall projection uncertainty in the Indo-Pacific domain, as the global averaged results in Fig. 7b may be the consequence of the cancelling effects of large regional differences.

Note that the globally averaged rainfall changes simulated in the *SST_exp* using ACCESS1.3 AGCM are consistently higher than the coupled runs (Fig. 7b). There are number of likely reasons for such results. First of all, studies (e.g. Cao et al. 2011; Richardson et al. 2016; Samset et al. 2016) showed that on global average CO_2 is a precipitation inhibitor through its impacts on atmospheric energy balance and thermal stratification while SST warming is

an enhancer. Thus, using SST warming from the models' coupled runs but with less increase in CO_2 concentration can lead to more global precipitation as reported by these studies. Another possible reason is that the SST climatologies are different in these nine models (SST climatology in ACCESS1.3 is warmer than others by about 0.15°C on average), so the same SST warming can result in higher SSTs used in ACCESS1.3 *SST_exp* and therefore generating more rainfall. Finally, we note that ACCESS1.3 has higher global model hydrological sensitivity ($\Delta P/\Delta T$) than most of the other eight models used in this study as assessed by Flaschner et al. (2016) so the same warming can lead to more rainfall increase in ACCESS1.3.

3.2 How much CMIP5 model disagreement in rainfall projection is linked to different SST warming?

Figure 8 shows the changes in DJF precipitation (%) simulated by the ACCESS1.3 *SST_exp* experiments (Table 1) using the SST warming simulated by these nine models. Precipitation anomalies are calculated against

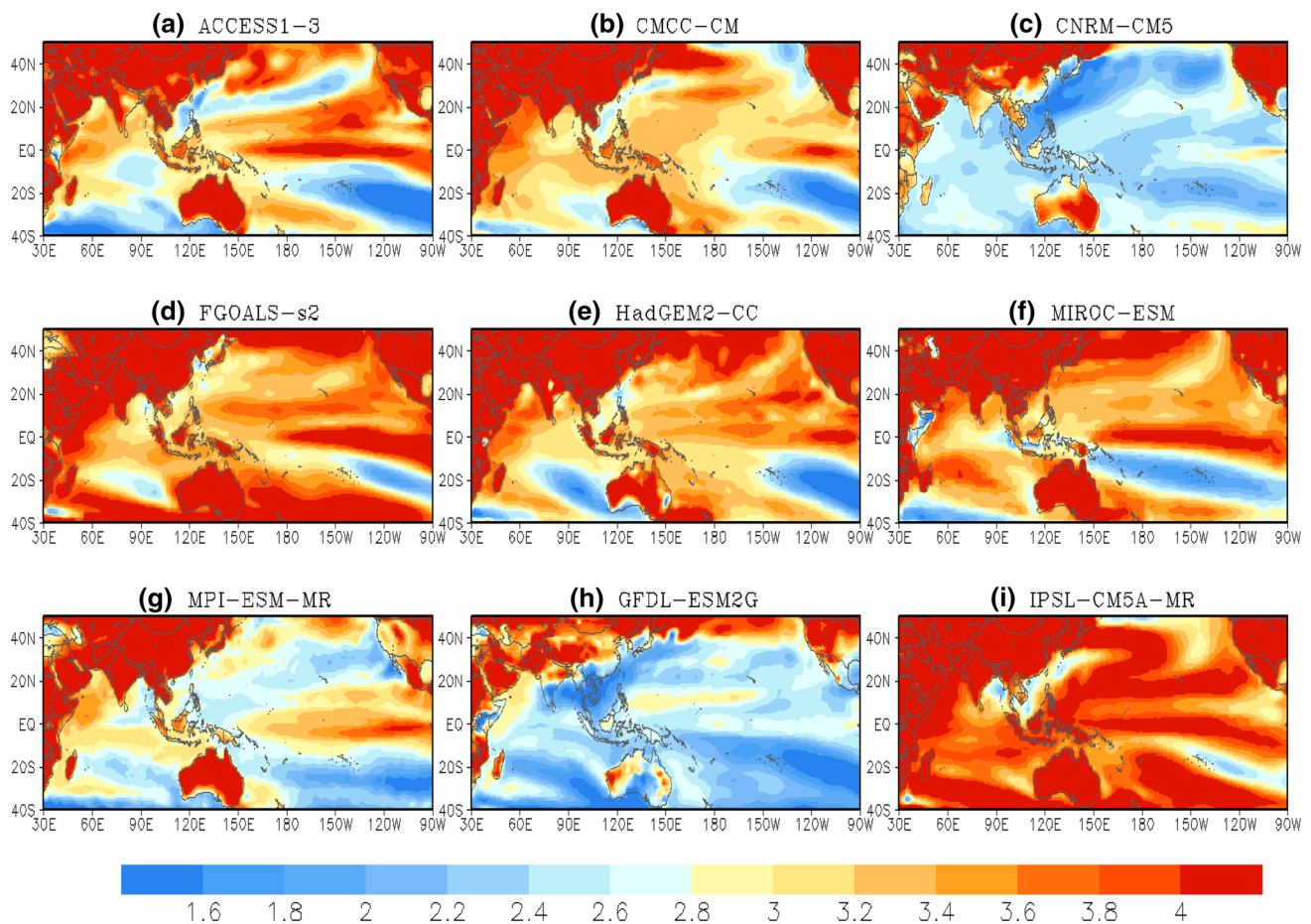


Fig. 6 Surface temperature warming anomalies ($^{\circ}\text{C}$) in DJF as simulated by the nine CMIP5 models in their coupled runs (see Table 1)

rainfall climatology in *ACCESSsst_his* (Table 1). Contrasting with their coupled results in Fig. 5, we can see following features:

1. The overall good agreement between rainfall changes from the *SST_exp* and fully coupled CMIP5 runs occurs over the eastern Pacific Ocean (roughly east of the dateline) and nearby land areas, where forcing ACCESS1.3 AGCM with different SST warming can largely reproduce the rainfall changes from the coupled runs. The pattern correlations between the two exceed 0.5 over the Indo-Pacific domain for the majority of the models. The dominant pattern includes enhanced rainfall over the tropical eastern Pacific, where most models simulate a larger SST warming than further west. This “warmer-get-wetter” pattern has been discussed by many studies (e.g., Xie et al. 2010; Trenberth 2011). Similar agreement among the nine models is also seen in other seasons (not shown). High SST-rainfall correlations in this region (Fig. 2) and the high similarity of rainfall changes between coupled runs and SST-forced
2. Another area where the *SST_exp* runs offer good agreement with the corresponding CMIP5 runs is in the western tropical Indian Ocean and extending toward the Arabian Sea and nearby tropical African continent. Of the nine models, eight of them (except for CNRM-CM5 in Figs. 5b, 8b) simulated significant rainfall increases in these regions and such changes are, by and large, reproduced in the *SST_exp* runs. Such results can also be partially attributed to strong air-sea coupling in the tropical western Indian Ocean, with results in both Figs. 1 and 2 showing observed and modelled SST-rainfall correlations much higher in the western Indian Ocean than to its east. Thus, superimposing SST warming anomalies in *SST_exp* can reproduce rainfall responses in this region too. Nevertheless, it is worthy pointing out that the model-simulated SST change patterns in the Indian Ocean may actually be spurious so

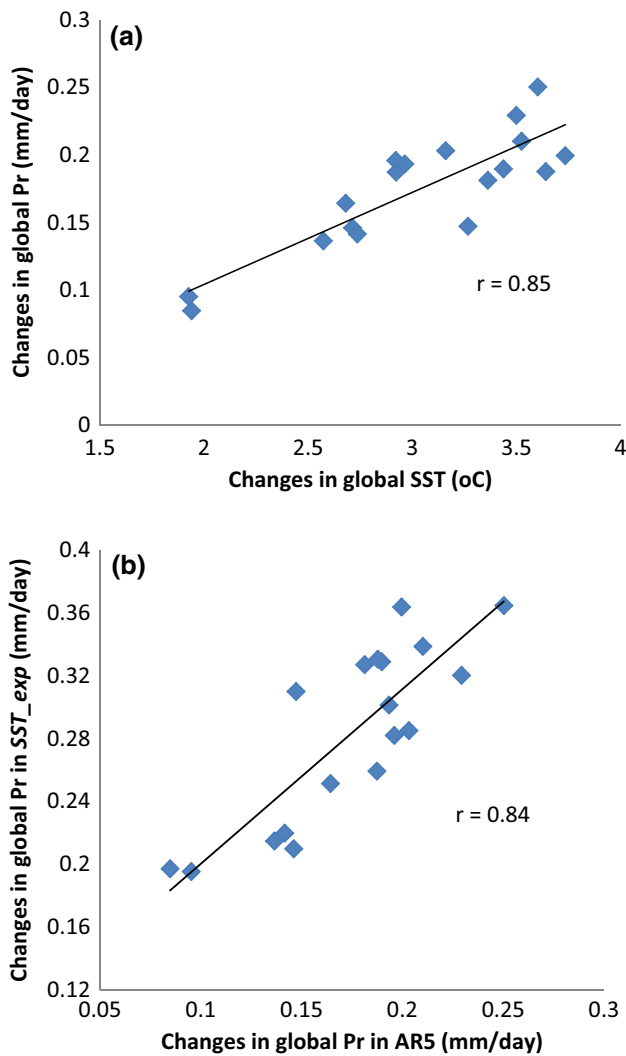


Fig. 7 **a** Correspondence of the nine model simulated global SST warming ($^{\circ}\text{C}$) and changes in global precipitation (mm d^{-1}) in their coupled CMIP5 experiments for DJF and JJA; **b** correspondence of the changes in global precipitation in their coupled CMIP5 experiments and the ones derived from nine *SST_exp* runs which force ACCESS1.3 AGCM with SST warming from nine coupled runs. Lines of best fit and correlation coefficients are also shown

the model agreement on precipitation changes in this region may also be spurious (Li and Xie 2016). Good inter-model agreement does not necessarily mean robust results.

3. The ACCESS1.3 AGCM *SST_exp* runs struggle to capture dominant rainfall patterns in the tropical western Pacific, Bay of Bengal, maritime continent and changes over the land areas including south and east Asia and Australian continent. For instance, the CMCC-CM coupled run (Fig. 5b) shows significant rainfall reductions in a large area of south and east Asia and a large part of the Australia continent and southern Indian Ocean. Such changes are not reproduced

in the *SST_exp* runs (Fig. 8b). Another example is the extensive rainfall increases in northern Indian Ocean, Bay of Bengal, south Asia and tropical western Pacific, and remarkable rainfall reductions across equatorial Indian Ocean in the *SST_exp* using SST warming from the MIROC-ESM (Fig. 8f). None of these is notable in its coupled CMIP5 results (Fig. 5f). The failure of ACCESS1.3 *SST_exp* runs here suggests complex air–sea and land–air interactions in these regions which determine how its rainfall varies with different underlying SST conditions. For instance, it is well-known that SST warming in the eastern Indian Ocean is the consequence of oceanic processes responding to the changes in atmospheric circulation and radiative forcing (Hendon et al. 2011; Zhang and Moise 2016). Therefore, over these regions, SST warming would not be expected to be the most dominant driving force for rainfall responses to global warming.

4. Of the nine models (apart from ACCESS1.3 model as documented in Sect. 2), HadGEM2-CC (Figs. 5e, 8e) offers the overall highest similarity of rainfall changes between *SST_exp* and its coupled runs over the whole Indo-Pacific domain. This is not surprising since these two models share strong similarities in their atmospheric model configurations (Bi et al. 2013; Martin et al. 2011), with the only main differences being their land-surface modelling components and treatment of clouds. Although the two CMIP5 models have very different ocean components (with ACCESS1.3 using the GFDL Modular Ocean Model 4 while HadGEM2-CC uses the Nucleus for European Modelling of the Ocean—NEMO) and the SST warming patterns differ between their CMIP5 runs (ref. Fig. 6a, e), using the SST warming from HadGEM2-CC in driving ACCESS1.3 AGCM can largely reproduce its rainfall change patterns. The only notable difference is over the Australian continent where its coupled runs simulated rainfall increases in the eastern parts of the continent and a drying in the west while the corresponding *SST_exp* run shows rainfall reductions broadly across the continent. The difference in land-surface modelling could be one of the reasons for such results. Besides the fact that the SST warming pattern in HadGEM2-CC is closest to ACCESS1.3 compared with the other models, it also highlights a significant role the atmospheric physics/dynamics can play in determining modelled rainfall responses to global warming. This will be expanded further below.

As a quantitative measure of rainfall similarities between coupled CMIP5 results and those from *SST_exp* experiments, we have calculated pattern correlations between the different sets of runs listed in Table 1. As

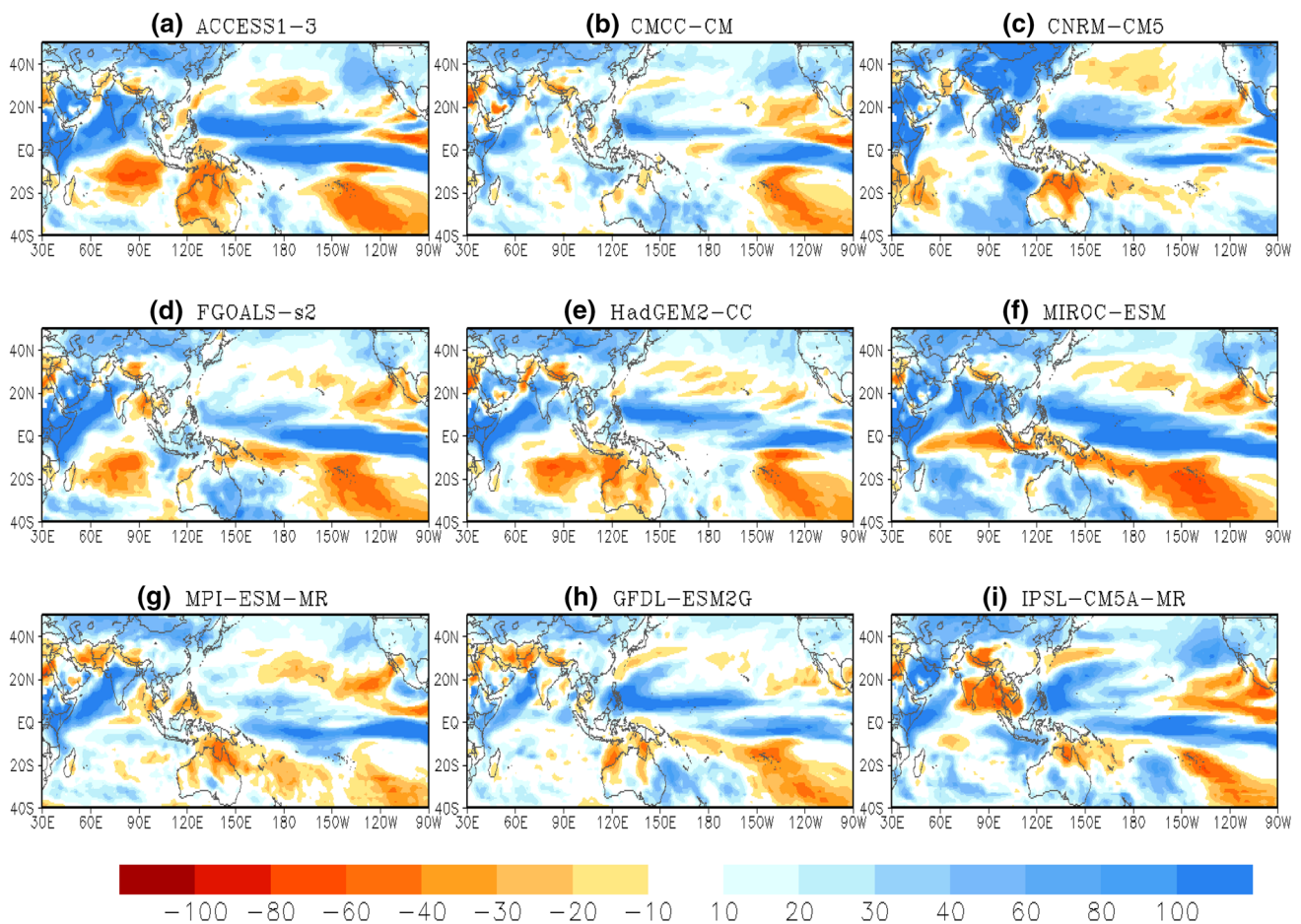


Fig. 8 Changes in DJF precipitation (%) simulated in the ACCESS1.3 *SST_exp* experiments as documented in Table 1. Changes are calculated against the rainfall climatology from

ACCESSsst_his experiment in which the ACCESS1.3 AGCM is forced by its coupled model-simulated SSTs for the period of 1971–2000

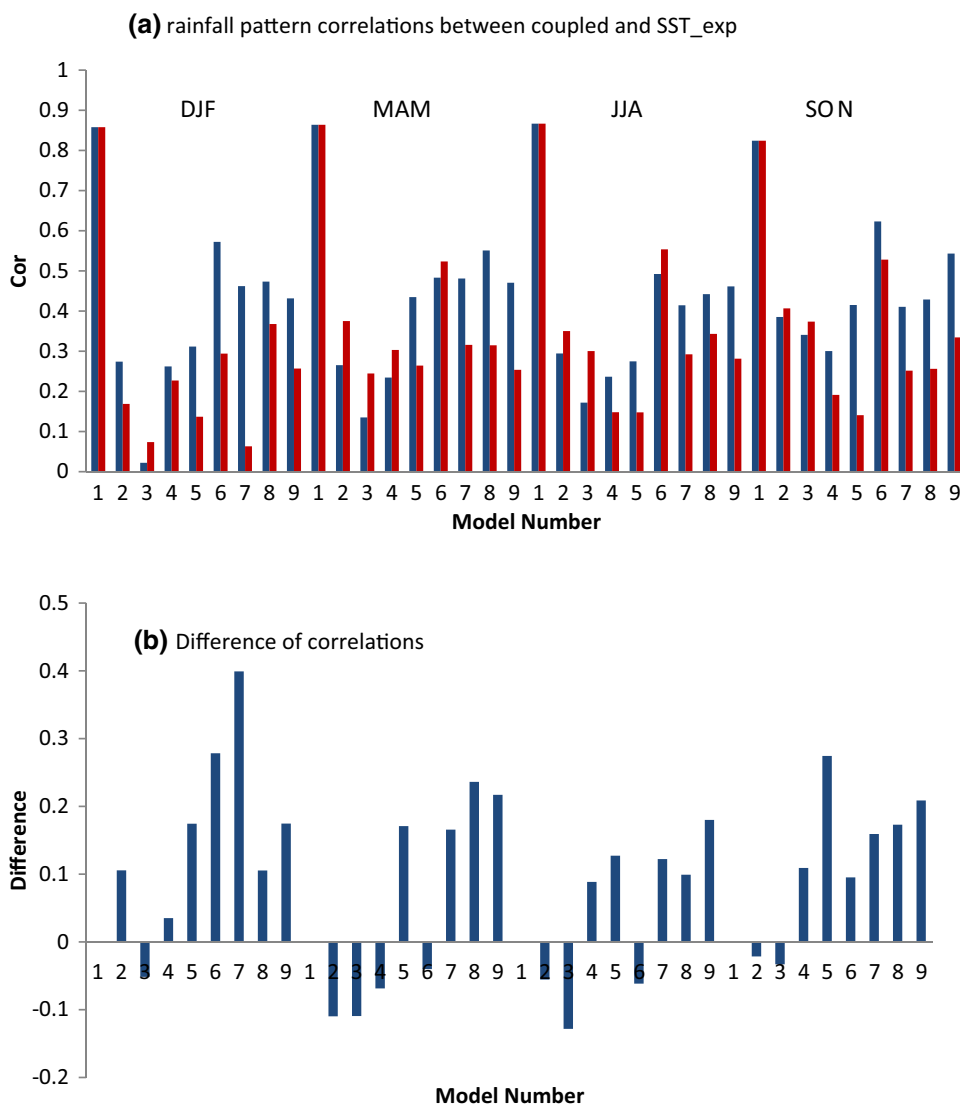
large uncertainties over the land are further complicated by different land-air coupling strengths in climate models (Koster et al. 2004), here we focus on results over oceanic grid-points only. Figure 9a compares the pattern correlations of rainfall changes in the tropical Indo-Pacific domain of 30–270°E; 30°S–30°N. The blue bars are the seasonally averaged pattern correlations between rainfall changes derived from each model’s CMIP5 runs (*RCP8.5* against *historical*: ref Table 1) and the ones derived from the corresponding *SST_exp* run using ACCESS1.3 AGCM. To complement the comparisons, the red bars show the pattern correlations of rainfall changes from each model’s coupled CMIP5 runs against rainfall changes derived from ACCESS1.3’s *SST_exp* runs. The rationale behind this one is that if uncertainty in the patterns of rainfall changes is not influenced by its SST warming patterns and/or intensities, we would expect similar results by forcing the AGCM either with its own SST warming or with other model’s. In this and following figures, the models are numbered from 1 to 9 in the order listed in Table 1. Note that such an analysis

is mainly for assessing the influence of uncertainty in SST pattern change on inter-model uncertainty in regional rainfall change, not the absolute influence of SST pattern change on regional rainfall change in a model in which case we need to compare results from each *SST_exp* experiment with a corresponding uniform SST warming experiment as used in He and Soden (2016).

In both the diagrams in Fig. 9, the correlations are shown for four seasons and for nine models. High correlation values are from ACCESS1.3 due to the fact that its *SST_exp* run reproduce its coupled results very well (ref Figs. 3, 4). From Fig. 9a, we can see:

1. The pattern correlations of rainfall changes between models’ *SST_exp* and their corresponding coupled runs in Indo-Pacific domain vary with models, with models No. 1, 6, 7, 8 and 9 (ACCESS1.3, HadGEM2-CC, IPSL-CM5A-MR, MIROC-ESM, and MPI-ESM-MR) giving higher correlations than the rest. The averaged pattern correlation for these models (excluding the

Fig. 9 Seasonally averaged pattern correlations of rainfall changes (ocean only) in the tropical Indo-Pacific domain (30–270°E; 30°S–30°N): **a** blue bars are the correlations between each model’s coupled run and its corresponding SST_exp run; red bars are the pattern correlations of rainfall changes in each model’s coupled run with the rainfall changes derived from ACCESS1.3 SST experiment (*ACCESSsst_rcp-ACCESSsst_his*). The models are numbered as in Table 1. **b** Differences of the correlations between the two in **a**



very high numbers of ~0.8 for ACCESS1.3) is about 0.45. This means about 20% of the rainfall pattern variance from these coupled models can be attributed to their SST warming. Note that in the results here the influence of different SST warming on regional rainfall change is separated out from the influence of different present-day SST climatologies and different model physics. It is possible that the influence of a particular model’s SST pattern change would be greater when it is combined with its baseline SST climatology and model physics, such as the results seen in ACCESS1.3 itself and results in a recent study of Chadwick et al. (2017). Therefore, the experiments used here could be viewed as a harsh test for the influence of SST patterns and the 20% contribution from the SST warmings can be viewed as a lower bound of such assessments. In addition, there may also be an upper bound due to the experimental design in this study as precipitation

changes in *ACCESSsst_rcp* experiment (ref. Table 1) has a correlation of around 0.85 with that of the ACCESS coupled model (ref. Fig. 7a), so an explained variance of around 70% may be the upper possible bound expected from these SST experiments. Overall, our experiments further demonstrate the complexity of understanding how uncertainty in tropical rainfall projections is linked to modelled SST warming which can be caused by different SST mean climate, different SST warming patterns/intensities and different atmospheric model physical responses to the underlying SST forcing.

- For most models the coupled model-simulated rainfall changes correlate more highly with *SST_exp* forced with its own SST warming (blue bars) than that with ACCESS1.3 SST warming (red bars). This re-confirms that in the tropical oceans, different SST warming contributes to the uncertainty in the modelled rainfall

changes. The differences between the two correlations (Fig. 9b) are generally higher in austral summer season and lower in the boreal summer season. This may be attributed to the complexity of the south Asian summer monsoon in which many processes contribute (ref. Wang 2006) so the relative dominance of SST influences diminishes.

When exploring rainfall projection uncertainty in CMIP5 models, Brown et al. (2015) emphasized the role of mean SST biases in the tropical western Pacific warm pool for regional rainfall changes. While, Chadwick (2016) and He and Soden (2016) discussed the contributions from SST warming patterns and SST biases leading to uncertainty in rainfall projections over tropical oceans. Figure 10 explores such connections in our experiments. In Fig. 10a, the x axis shows correlations of monthly mean SST climatologies in the nine CMIP5 models with the ACCESS1.3

SST climatology in their coupled *historical* runs. Plotted against this are the pattern correlations between coupled model rainfall changes and changes simulated by the *SST_exp* runs as shown in Fig. 9a. In each of the diagrams of Fig. 10, we show two correlation coefficients for the inter-model scatters. r_9 refers to the correlation calculated when all the nine models are used. The results from ACCESS1.3 are included to be as a reference to show pattern correlations of rainfall changes in its coupled and uncoupled runs with identical SST warming. r_8 refers to the correlation calculated without ACCESS1.3 itself. Figure 10a clearly suggests that for models with more similar tropical SST spatial patterns in their *historical* runs to ACCESS1.3, super-imposing their simulated SST warming onto SSTs from ACCESS1.3 *historical* run provides better simulations of their coupled model rainfall projections than for the models whose SST climatology patterns are less similar to ACCESS1.3. The correspondence between the

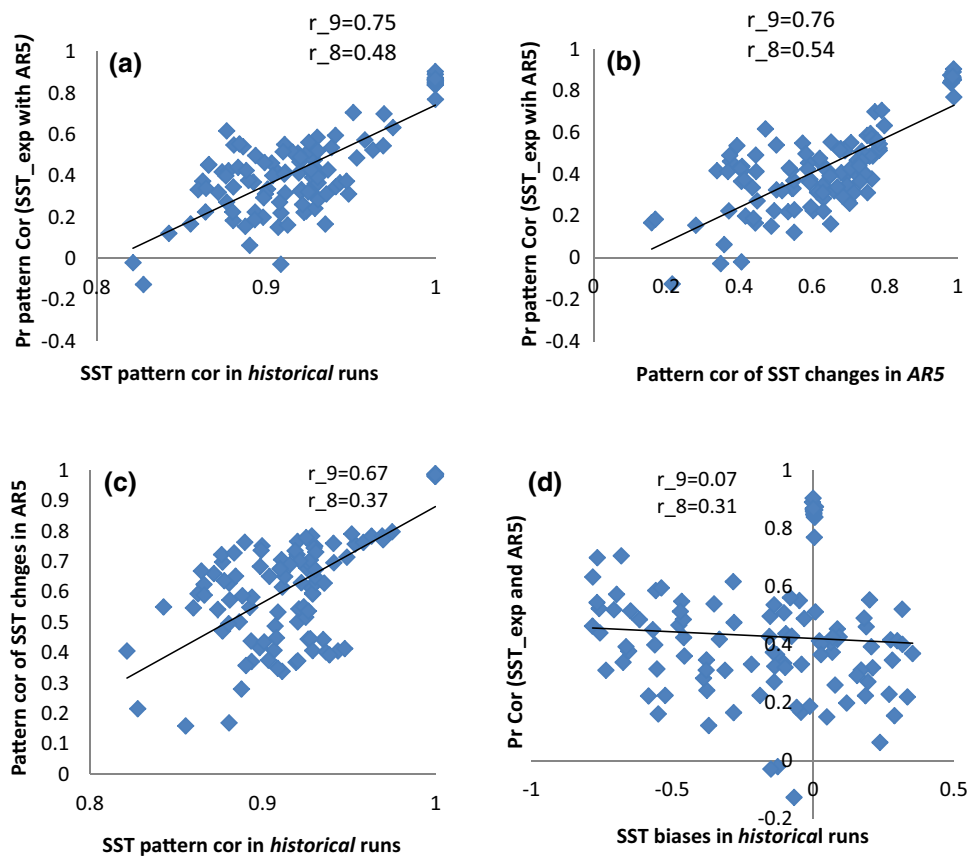


Fig. 10 **a** Correspondence of the pattern correlations of the nine models’ SST climatologies with ACCESS1.3 in their historical runs (*x-axis*) with the pattern correlations of rainfall changes derived from the nine models’ coupled results (*RCP8.5-historical*) and their corresponding *SST_exp* results (*SST_exp-ACCESSsst_his*) (*y-axis*); **b** as **a** but the *x-axis* becomes the pattern correlations of changes in SST in their coupled historical runs with ACCESS1.3; **c** as **a** but the *y-axis* becomes the pattern correlations of changes in SST in their coupled

historical runs with ACCESS1.3; **d** as **a** but the *x-axis* becomes the SST mean biases against ACCESS1.3 in their coupled historical runs (°C). All the results are for the Indo-Pacific domain (30–270°E; 30°S–30°N). Lines of best fit and two correlations are also shown. r_9 refers to the correlation calculated when all the nine models are included while r_8 refers to the correlation when ACCESS1.3 is excluded in the calculations

two has a correlation coefficient of 0.75 when all the nine models are accounted. Excluding results from ACCESS1.3 yields a correlation of 0.48 and such an association is much clearer than the results for area-averaged SST biases shown in Fig. 10d. To further assess the influence of SST warming patterns, Fig. 10b plots out the correspondence for the pattern correlations between rainfall changes in coupled and *SST_exp* runs as in Fig. 10a (y-axis) against pattern correlations of SST changes simulated by these coupled model AR5 runs against ACCESS1.3 (x-axis). Similarly, the result suggests that if the SST warming patterns are closer in their coupled experiments, forcing ACCESS1.3 AGCM with these simulated SST warming can reproduce well the rainfall changes in their coupled experiments. Again, this underlines the important role of SST warming patterns for leading to uncertainty in the model rainfall projections. The fact that in Fig. 10b precipitation change from a given model is better reproduced by the ACCESS1.3 AGCM if SST pattern changes are similar between the two could be due to one of two factors: (a) SST pattern change in each model is related to its historical SST pattern as discussed in Brown et al. (2015). Therefore if SST pattern change in a model is similar to ACCESS1.3, its historical SST pattern is also similar to ACCESS1.3; (b) ACCESS1.3 atmospheric physics are able to produce a more similar precipitation response when SST pattern change from a given model is similar to the ACCESS1.3 SST pattern change. To further examine these two likely reasons, in Fig. 10c we plot out climatological SST pattern correlations in their coupled CMIP5 runs to ACCESS1.3 against the pattern correlations of SST warmings simulated by these models compared to ACCESS1.3. Indeed, there is a degree of connection between two, with a correlation coefficient being about 0.37 for the eight models excluding ACCESS1.3 itself (Fig. 10c). This supports the argument in Brown et al. (2015) that coupled model SST warming biases are partly linked to its baseline climatological biases. This explains part of the similarity between Fig. 10a, b. The other reason is that our ACCESS1.3 AGCM experiments tend to suggest a bigger role of SST warming patterns in explaining inter-model difference than SST biases. This is further complemented by Fig. 10d in which the x-axis is now replaced by area-averaged mean SST biases (calculated as the area-averaged SST difference over the Indo-Pacific domain between the coupled *historical* runs against the one from ACCESS1.3 *historical* run). The models with smaller systematic SST biases against ACCESS1.3 in their *historical* runs do not show a better duplication of rainfall changes from their coupled run by forcing ACCESS1.3 AGCM with their SST warming. The scatters among these models are overall flat in Fig. 10d. Excluding ACCESS1.3 model results, it even shows a weak linear tendency (with correlation coefficient of 0.31) that models with cooler SST

biases may even have a higher rainfall pattern correlations between their coupled run and the one from ACCESS1.3 *SST_exp* run. Although our experimental results shown from Fig. 10 suggest SST warming patterns are more influential than SST biases in causing the inter-model difference, we acknowledge that the SST biases here are only area-averaged mean biases. We did not consider the spatial patterns of such SST biases as studied in He and Soden (2016) in which they also underlined the importance of SST patterns in explain inter-model variations in their regional rainfall projections while considered the spatial distribution of the SST biases.

While the results here demonstrate the contributions of different SST warming leading to uncertainties in rainfall projections, we must also emphasise the importance of fundamental atmospheric dynamics and physics as well. Figure 8 has already shown a degree of similarity in the patterns of rainfall changes derived from the nine *SST_exp* runs. To help quantify the role of model physics in model discrepancies, Fig. 11 (blue bars) shows seasonally averaged pattern correlations between rainfall changes derived from the eight *SST_exps* with the one derived from ACCESS1.3 SST runs. If atmospheric model physics is important in determining rainfall projections, one would expect a high similarity among the ACCESS1.3 *SST_exps* regardless of which SST warming is used in forcing this model. Indeed, high correlations (around 0.5 and above) exist, in particular for model No. 3 (CNRM-CM5), 5 (GFDL-ESM2G), 6 (HadGEM2-CC), 8 (MIROC-ESM) and 9 (MPI-ESM-MR). Their projected SST warming patterns and intensities differ quite markedly at regional scales as shown in Fig. 6. Yet, using them to force a single host AGCM with the same model physics/dynamics, it yields similar precipitation changes. Such correlations are much higher than the correlations of rainfall changes simulated in the coupled runs as red bars (different model physics responding to these different SST warming). Combining the results from Figs. 9 and 10 further underlines that SST warming patterns/intensity are only part of the causes of the uncertainty in the models. It is equally important to recognize uncertainty caused by different model physics/dynamics and different atmospheric circulation responses to the SST warming (Colman et al. 2011; Moise et al. 2012; Shepherd 2014).

Besides SST warming, in the *SST_exp* runs the ACCESS1.3 AGCM is also constrained by enhanced GHG radiative forcing. One may argue that the enhanced radiative forcing applied in the model may have overshadowed the impacts of different SST warming. To test this we conducted and examined the *SSTghg_exp* experiments (Table 1) in which GHG concentrations were set as in the CMIP5 *historical* run settings (Taylor et al. 2012). Figure 12 compares the pattern correlations derived from

Fig. 11 **a** Blue bars show seasonally averaged pattern correlations between the rainfall changes derived from 9 SST_exp runs (*SST_exp-ACCESSsst_his*) and the changes derived from ACCESS1.3 SST_exp (*ACCESSsst_rep-ACCESSsst_his*); red bars show the correlations in their coupled CMIP5 results against the ACCESS1.3 coupled results. All results are for the Indo-Pacific domain. **b** Differences between the two correlations

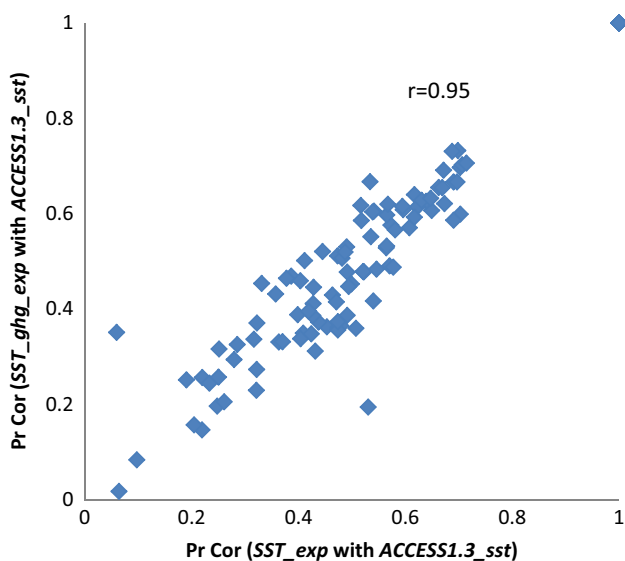
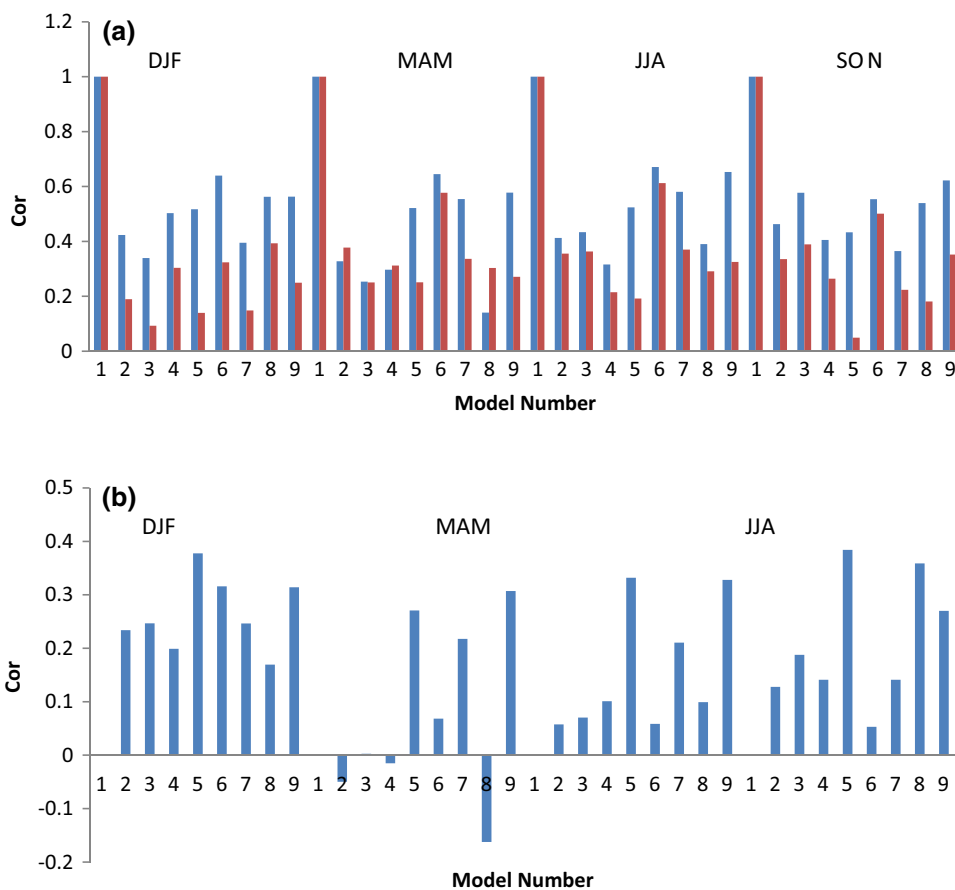


Fig. 12 Pattern correlations of rainfall changes in the Indo-Pacific domain. X-axis corresponds to the changes derived from *SST_exp* results (against *ACCESSsst_his*) against changes derived from ACCESS1.3 SST runs (*ACCESSsst_rep-ACCESSsst_his*). Y-axis corresponds to the changes derived from *SSTghg_exp* results (against *ACCESSsst_his*) against changes derived from ACCESS1.3 SST runs (*ACCESSsst_rep-ACCESSsst_his*). Correlation coefficient is also included

◆ *SSTghg_exp* runs with the ones derived from *SST_exp* runs and clearly they are very similar, with a correlation coefficient of 0.95. These results suggest that the similarity of rainfall change patterns in the ACCESS1.3 AGCM *SST_exp* experiments in Fig. 11 is not likely to be constrained by the enhanced GHG radiative forcing imposed.

To further demonstrate that model physics/dynamics employed in these models and their responses to different SST patterns are important for understanding the uncertainty in current rainfall projections at regional scale, Fig. 13 shows the averaged correlations between January tropical zonal winds with the model-simulated Nino3.4 index in the nine models in their coupled *historical* runs. This is a basic measure of how the large-scale tropical circulation responds to SST forcing in the tropical central-eastern Pacific. Although very broad features are, to some extent, comparable among the models, there are notable differences in details. For instance, they show large discrepancies in the extent and the location of the westerly wind anomalies in the central-west tropical Pacific. Models including ACCESS-1.3, GFDL-ESM2G, HadGEM2-CC, IPSL-CM5A-MR and MPI-ESM-MR show much wider longitudinal coverage than the narrow

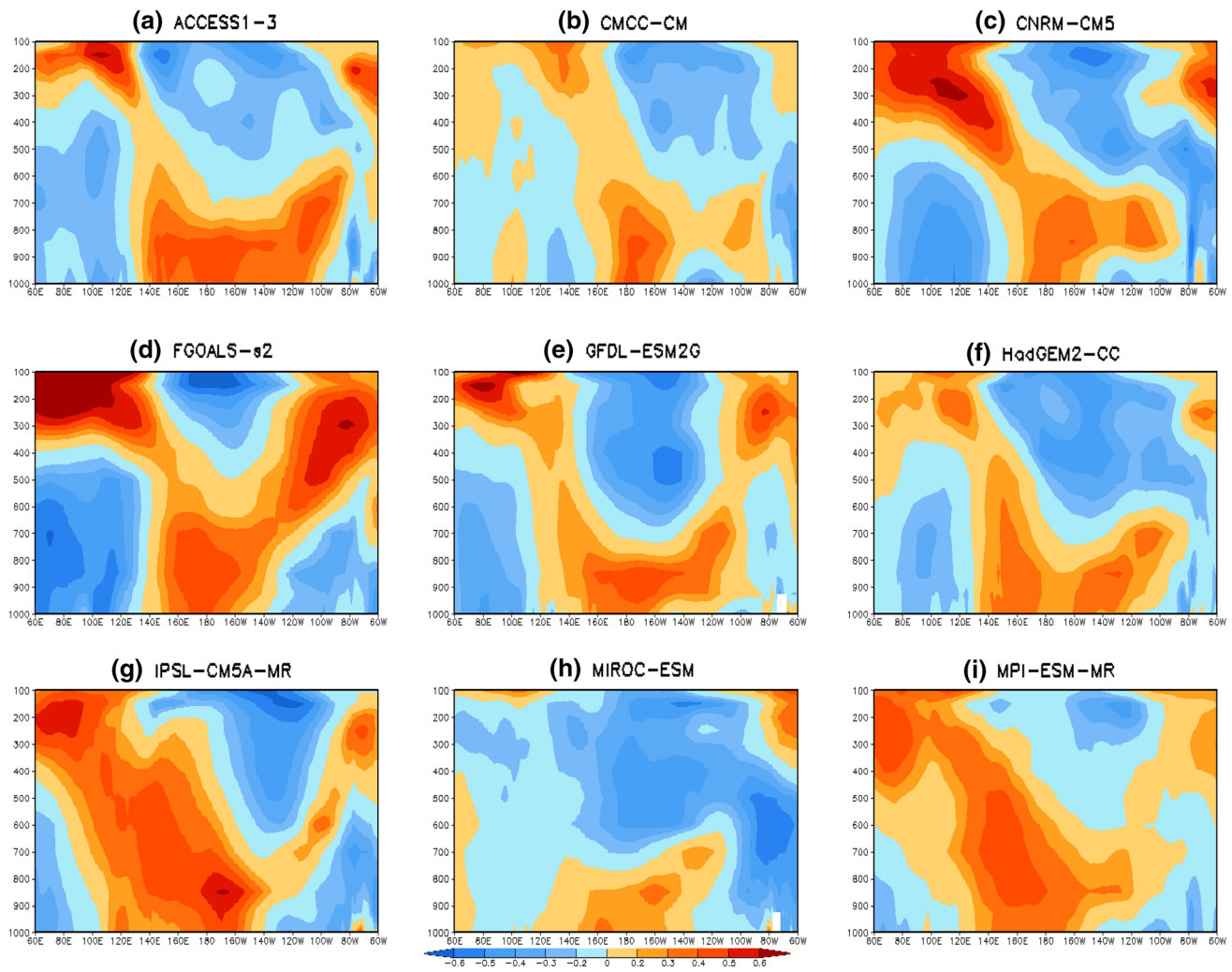


Fig. 13 Vertical profiles of the averaged correlations (10°S – 10°N) between zonal wind and Nino3.4 index (area-averaged SST anomalies over 190 – 240°E , 5°S – 5°N) simulated by the nine CMIP5 models in

their coupled historical runs in January for the period of 1950–2004 (unit: dimensionless). Warm/cool colours indicate enhanced/weakened westerlies with warmer NINO3.4 SSTs

ones in CMCC-CM, CNRM-CM5, FGOALS-s2 and MIROC-ESM. The positive/negative correlations correspond to enhanced horizontal zonal wind convergence/divergence. Responding to SST warming in Nino3.4, several models have enhanced low-level convergence and high-level divergence right over the tropical central Pacific—around 180 – 220°E (CMCC-CM, CNRM-CM5, FGLAOLS-s2, MPI-ESM-MR), while others (ACCESS1.3, GFDL-ESM2G, HadGEM2-CC, MIROC-ESM) have ascending enhanced to the far tropical eastern Pacific. Large differences can also be seen in the tropical western Pacific—around 110 – 160°E . All these differences can result in different rainfall responses to the same SST warming in the central-eastern Pacific, lead to the uncertainty in the model projected rainfall changes in the tropical regions.

4 Conclusion and discussions

Understanding and narrowing the causes of uncertainty in current global climate model rainfall projections is a key area in climate change modelling. A large number of studies have emphasised the importance of different SST warming in projected rainfall changes either through comprehensive CMIP5 model analyses (Xie et al. 2010; Chadwick et al. 2013, 2014; Grose et al. 2014; Kent et al. 2015; Brown et al. 2016; Chadwick 2016), or through model experimentation (Zhou et al. 2014; Zhou and Xie 2015; Brown et al. 2015; He and Soden 2016; Chadwick et al. 2017). Nevertheless, other studies (Colman et al. 2011; Moise et al. 2012; Shepherd 2014) highlight the uncertainty caused by differences in simulating how atmospheric circulation and/or convections responses to global warming. In this study we have conducted a series of SST

experiments using a single AGCM (ACCESS1.3, Bi et al. 2013) to estimate the contributions of different SST warming to discrepancies in model-projected rainfall changes in the Indo-Pacific domain.

Based on our previous CMIP5 monsoon studies (Dong et al. 2015; Zhang et al. 2016), nine CMIP5 model-simulated global SST warming anomalies were selected, and super-imposed onto the SSTs simulated by ACCESS1.3 coupled *historical* run. Such experiments are complementary to some previous studies discussed above as here we have applied SST warming anomalies from different CMIP5 model simulations to the same AGCM—in contrast to the same SST warming applied to different AGCMs as in studies by Zhou et al. (2014) and Zhou and Xie (2015), or the same SST warming applied to different model SST climatologies (He and Soden 2016). Using a different AGCM, our results help to examine whether results reported in studies such as He and Soden (2016) are model-dependent.

At global scales there is good correlation between model-simulated global SST warming intensities and the globally averaged changes in precipitation, explaining about 70% the spread among the models. Superimposing SST warming patterns onto the ACCESS1.3 *historical* SSTs can largely reproduce the spread of globally-averaged rainfall changes in the fully coupled CMIP5 runs. Nevertheless, there are significant *regional* variations in attributing uncertainty in modelled rainfall changes in the Indo-Pacific region to different SST warming. Over tropical eastern Pacific and western Indian Ocean where SST-rainfall coupling is strong, ACCESS1.3 *SST_exp* runs reasonably reproduce coupled model results. However, this is less the case over the tropical western Pacific, south Asian monsoon region and Australian continent. Pattern correlations between SST-forced (*SST_exp*) and fully coupled model results are around 0.45 for over half of the models, implying that SST warming explains about 20–25% of the patterns of precipitation changes in each of the four/five models in its rainfall projections over the oceans in the Indo-Pacific domain. There are also a couple of models showing very weak influence. Such results from our study could be due to the fact that we applied different SST warming anomalies to the same current-climate SSTs in each case. Given the fact that significant SST climatological biases exist among the climate models, the same SST warming can have different effects when super-imposed on to different climatology as reported in He and Soden (2016). Our analysis further finds that different SST warming patterns have more impacts than areal-averaged systematic SST mean biases, supporting the findings from He and Soden (2016) and Chadwick (2016) from a different point of view. Nevertheless, another useful set of experiments would be valuable to further separate the contributions from SST warming anomalies and SST mean biases by forcing ACCESS1.3

AGCM with future SSTs rather than SST warming anomalies. Such experiments are in preparation in our future modelling experiments.

On the other hand, we also underlined the importance of different atmospheric physics/dynamics employed across the CMIP5 models in causing the model uncertainty. Of the nine models (apart from itself), we found ACCESS1.3 *SST_exp* run tend to be most successful in reproducing the coupled results from HadGEM2-CC despite of the fact that they used different ocean models and there are differences in their simulated SST warming (ref. Fig. 6). Although SST warming patterns between these two models are closer than other models (with correlation coefficients being around 0.75), we also attribute part of the results to the close atmospheric model configurations used in both models. As a result, the patterns of SST-rainfall correlations in Fig. 2 and SST-wind correlations in Fig. 13 share very similar features between these two models. This highlights the importance of different atmospheric circulation responses to SST warming in causing rainfall uncertainties. Our results further showed that the models differed significantly at regional scale in modelling how the large-scale tropical Walker circulation responds to SST warming in the Nino3.4 region.

Finally, we must acknowledge a number of caveats in our study. The first one is that our results may be model dependent. Our results showed that models have different air-sea coupling strengths and ACCESS1.3 tends to have a stronger rainfall response to tropical SSTs. It would be desirable to apply the same approach to a series of AGCMs to confirm the results from this study and the ones reported by He and Soden (2016). Secondly, significant biases exist among the CMIP5 model SST climatologies (Brown et al. 2015, 2016) and the same SST warming can have different effects on rainfall projections if these anomalies are applied to different SST climatologies (such as Zhou and Xie 2015). Therefore, it is also desirable to apply the SST warming to a different SST time series from another model's CMIP5 historical runs, or by forcing the same AGCM with model-simulated SSTs in warmed climate. Although it is impossible to cover all these aspects in one study, they are considered in our future modelling experiments.

Acknowledgements Part of the analysis was conducted when Dr. Yong Zhao visited the Bureau of Meteorology (BoM) in January–March 2015 under a BoM–CMA bilateral agreement on climate change collaborations. The study was also partially supported by the Australian Climate Change Science Programme, a collaboration between the Bureau of Meteorology, CSIRO and the Department of the Environment. We acknowledge the World Climate Research Programme's Working Group on Coupled Modelling, which is responsible for CMIP, and the climate modelling groups (see Table 1) for producing and making available their model output. For CMIP the US Department of Energy's PCMDI provides coordinating support and led development of software infrastructure in partnership with the

Global Organization for Earth System Science Portals. We acknowledge thoughtful comments and suggestions from Drs. Jo Brown, Hongyan Zhu and Tony Hirst during the internal review process. Very thoughtful and constructive comments from the two anonymous reviewers are much appreciated. Inquiries for model and analysis data in this study should be directed to the corresponding author.

References

- Allen MR, Ingram WJ (2002) Constraints on future changes in climate and the hydrologic cycle. *Nature* 419:224–232
- Bi D et al (2013) The ACCESS coupled model: description, control climate and evaluation. *Aust Meteorol Oceanogr J* 63:41–64
- Bollasina M, Nigam S (2009) Indian Ocean SST, evaporation, and precipitation during the South Asian summer monsoon in IPCC-AR4 coupled simulations. *Clim Dyn* 33:1017–1032
- Brown, JR, Moise AF, Colman RA (2013), The South Pacific convergence zone in CMIP5 simulations of historical and future climate. *Clim Dyn* 41:2179–2197
- Brown JN, Matear R, Brown JR, Katzfey J (2015) Precipitation projections in the tropical Pacific are sensitive to different types of SST bias adjustment. *Geophys Res Lett* 42:10856–10866
- Brown J, Moise A, Colman R, Zhang H (2016) Will a warmer world mean a wetter or drier Australian monsoon? *J Clim*. doi:10.1175/JCLI-D-15-0695.1
- Cao L, Bala G, Caldeira K (2011) Why is there a short-term increase in global precipitation in response to diminished CO₂ forcing? *Geophys Res Lett*. doi:10.1029/2011GL046713
- Chadwick R (2016) Which aspects of CO₂ forcing and SST warming cause most uncertainty in projections of tropical rainfall change over land and ocean? *J Clim* 29:2493–2509
- Chadwick R, Boutle I, Martin G (2013) Spatial patterns of precipitation change in CMIP5: why the rich do not get richer in the tropics. *J Clim* 26:3803–3822
- Chadwick R, Good P, Andrews T, Martin G (2014) Surface warming patterns drive tropical rainfall pattern responses to CO₂ forcing on all timescales. *Geophys Res Lett* 41:610–615
- Chadwick R, Douville H, Skinner C (2017) Timeslice experiments for understanding regional climate projections: applications to the tropical hydrological cycle and European winter circulation. *Clim Dyn*. doi:10.1007/s00382-016-3488-6
- Colman RA, Moise AF, Hanson L (2011) Tropical Australian climate and the Australian monsoon as simulated by 23 CMIP3 models. *J Geophys Res* 116:D10116
- Curry JA, Webster PJ (2011) Climate science and the uncertainty monster. *Bull Am Meteorol Soc*. doi:10.1175/2011BAMS3139.1
- Dong G, Zhang H, Moise A, Hanson L, Liang P, Ye H (2015) CMIP5 model-simulated onset, duration and intensity of the Asian summer monsoon in current and future climate. *Clim Dyn*. doi:10.1007/s00382-015-2588-z
- Flaschner D, Mauritsen T, Stevens B (2016) Understanding the intermodal spread in global-mean hydrological sensitivity. *J Clim* 29:801–817
- Grose MR, Bhend J, Narsey S, Sen Gupta A, Brown JR (2014) Can we constrain CMIP5 rainfall projections in the tropical Pacific based on surface warming patterns? *J Clim*. doi:10.1175/JCLI-D-14-00190.1
- Hawkins E, Sutton R (2011) The potential to narrow uncertainty in projections of regional precipitation change. *Clim Dyn* 37:407. doi:10.1007/s00382-010-0810-6
- He J, Soden BJ (2016) The impact of SST biases on projections of anthropogenic climate change: a greater role for atmosphere-only models? *Geophys Res Lett* 43:7745–7750
- Held IM, Soden BJ (2005) Robust responses of the hydrological cycle to global warming. *J Clim* 19:5686–5699
- Hendon HH, Lim E, Wheeler MC (2011) Seasonal prediction of Australian summer monsoon rainfall. In: Chang CP, Ding YH, Lau NC, Johnson R, Wang B, Yasunari T (eds), *The global monsoon system: research and forecast*, 2nd edn. World Scientific Series on Asia–Pacific Weather and Climate, vol 5, pp 73–84
- Hewitt HT, Copesey D, Culverwell ID, Harris CM, Hill RSR, Keen AB, McLaren AJ, Hunke EC (2011) Design and implementation of the infrastructure of HadGEM3: the next-generation Met Office climate modelling system. *Geosci Model Dev* 4:223–253
- Huffman GJ, Adler RF, Bolvin DT, Gu G (2009) Improving the global precipitation record: GPCP version 2.1. *Geophys Res Lett* 36:L17808
- IPCC (Intergovernmental Panel on Climate Change) (2007) *Climate change 2007: the physical science basis*. In: Solomon S (ed) Contribution of working group I to the fourth assessment report of the IPCC. Cambridge Univ. Press, Cambridge
- IPCC (Intergovernmental Panel on Climate Change) (2013) *Climate change 2013: the physical science basis*. In: Stocker T et al (ed) Contribution of working group I to the fifth assessment report of the IPCC. Cambridge Univ. Press, Cambridge
- Kent C, Chadwick R, Powell DP (2015) Understanding uncertainties in future projections of seasonal tropical precipitation. *J Clim* 28:4390–4413. doi:10.1175/JCLI-D-14-00613.1
- Koster RD et al (2004) Regions of strong coupling between soil moisture and precipitation. *Science* 305:1138–1140
- Kowalczyk EA, Stevens L, Law RM, Dix M, Wang YP, Harman IN, Hayens K, Sribnovsky J, Pak B, and Zhien T (2013) The land surface model component of ACCESS: description and impact on the simulated surface climatology. *Aust Met Oceanogr J* 63:65–82
- Lavers DA, Ralph FM, Waliser DE, Gershunov A, Dettinger MD (2015) Climate change intensification of horizontal water vapour transport in CMIP5. *Geophys Res Lett* 42:5617–5625
- Li G, Xie S-P (2016) A robust but spurious pattern of climate change in model projections over the tropical Indian Ocean. *J Clim* 29:5589–5608
- Martin GM et al (2011) The HadGEM2 family of Met Office Unified Model climate configurations. *Geosci Model Dev* 4:723–757
- Moise AF, Colman RA, Brown JR (2012) Behind uncertainties in projections of Australian tropical climate: analysis of 19 CMIP3 models. *J Geophys Res* 117:D10103. doi:10.1029/2011JD017365
- Richardson TB, Forster PM, Andrews T, Parker DI (2016) Understanding the rapid precipitation response to CO₂ and aerosol forcing on a regional scale. *J Clim* 29:583–594
- Samset BH et al (2016) Fast and slow precipitation responses to individual climate forcers: a PDRMIP multimodel study. *Geophys Res Lett* 43:2782–2791
- Shepherd TG (2014) Atmospheric circulation as a source of uncertainty in climate change projections. *Nat Geosci* 7:703–708
- Smith TM, Reynolds RW (2003) Extended reconstruction of global sea surface temperatures based on COADS data (1854–1997). *J Clim* 16:1495–1510
- Song X, Zhang GJ (2014) Role of climate feedback in El Niño-like SST response to global warming. *J Clim* 27:7301–7318
- Taylor KE, Stouffer RJ, Meehl GA (2012) An overview of CMIP5 and the experiment design. *Bull Am Met Soc* 93:485–498. doi:10.1175/BAMS-D-11-00094.1
- Trenberth KE (2011) Changes in precipitation with climate change. *Clim Res* 47:123–138
- Wang B (2006) *The Asian monsoon*. Springer, Heidelberg
- Watterson I, Hirst A, Rotstayn L (2013) A skill score based evaluation of simulated Australian climate. *Aust Met Oceanogr J* 63:181–190

- Wilson DR, Bushell AC, Kerr-Munslow AM, Price JD, Morcrette CJ (2008) PC2: a prognostic cloud fraction and condensation scheme. I: Scheme description. *Q J R Meteorol Soc* 134:2093–2107
- Xie SP, Deser C, Vecchi GA, Ma J, Teng H, Wittenberg AT (2010) Global warming pattern formation: sea surface temperature and rainfall. *J Clim* 23:966–986
- Yeh SW, Ham YG, Lee JY (2012) Changes in the tropical Pacific SST trend from CMIP3 to CMIP5 and its implication of ENSO. *J Clim* 25:7764–7771
- Zhang H (2010) Diagnosing Australia–Asian monsoon onset/retreat and using large-scale wind and moisture indices. *Clim Dyn* 35:601–618
- Zhang H, Moise A (2016) The Australian summer monsoon in current and future climate. In: de Carvalho LMV, Jones C (eds) *The monsoons and climate change*. Springer, Berlin, pp 67–120
- Zhang H, Liang P, Moise A, Hanson L (2012) Diagnosing potential changes in Asian summer monsoon onset and duration in IPCC AR4 model simulations using moisture and wind indices. *Clim Dyn* 39:2465–2486
- Zhang H, Moise A, Liang P, Hanson L (2013) The response of summer monsoon onset/retreat in Sumatra-Java and tropical Australia region to global warming in CMIP3 models. *Clim Dyn* 40:377–399
- Zhang H, Dong G, Moise A, Colman R, Hanson L, Ye H (2016) Uncertainty in CMIP5 model-projected changes in the onset/retreat of the Australian summer monsoon. *Clim Dyn* 46:2371–2389
- Zhao Y, Zhang H (2016) Impacts of SST warming in tropical Indian Ocean on CMIP5 model-projected summer rainfall changes over Central Asia. *Clim Dyn* 46:3223. doi:[10.1007/s00382-015-2765-0](https://doi.org/10.1007/s00382-015-2765-0)
- Zhou Z-Q, Xie S-P (2015) Effects of climatological model biases on the projection of tropical climate change. *J Clim* 28:9909–9917
- Zhou Z-Q, Xie S-P, Zheng X-T, Liu Q, Wang H (2014) Global warming-induced changes in El Niño teleconnections over the North Pacific and North America. *J Clim* 27:9050–9064